

DOI: 10.1007/s11430-006-0731-8

Grain-size features of a Miocene loess-soil sequence at Qinan: Implications on its origin

QIAO Yansong^{1,3}, GUO Zhengtang^{2,1}, HAO Qingzhen¹, YIN Qiuzhen¹, YUAN Baoyin¹ & LIU Tungsheng¹

1. Institute of Geology and Geophysics, Chinese Academy of Sciences, Beijing 100029, China;

2. Institute of Earth Environment, Chinese Academy of Sciences, Xi'an 710075, China;

3. Institute of Geomechanics, Chinese Academy of Geological Sciences, Beijing 100081, China

Correspondence should be addressed to Guo Zhengtang (email: ztguo@mail.iggcas.ac.cn)

Received November 15, 2005; accepted March 7, 2006

Abstract In this study, grain-size of 507 bulk samples from the QA-I Miocene loess-soil sequence at Qinan were analyzed, and the grain-size features are compared with those of typical Quaternary loess and soil samples, representative lacustrine and fluvial samples. The results indicate that the grain-size distribution pattern of the Miocene loess is essentially similar to that of Quaternary loess, but greatly differs from the lacustrine and fluvial sediments. Loess layers are regularly coarser than soil layers, indicating cyclical climate changes. Median grain-size along the 253.1 m sequence varies from 6 to 13 μm and the $>63 \mu\text{m}$ fraction represents only 5.3% in maximum, 0.9% in average. Long-term grain-size variations are consistent with the loess accumulation rate at Qinan and with the eolian mass accumulation rate in the North Pacific. These features firmly indicate an eolian origin of the studied sequence, and also reveal a coeval changes between the long-term changes of eolian grain-size and continental aridity in the dust source regions.

Keywords: Qinan, Miocene loess-soil sequence, grain-size, eolian origin.

In northern China, the Quaternary loess-soil sequences^[1] and the *Hipparion* Red-Earth Formation in the eastern Loess Plateau^[2-6] provide a continental climate record for the past 8 Ma. The recently reported Miocene^[7] and Pliocene^[8] loess-soil sequences near Qinan constitute an eolian record of the western Loess Plateau from 22 to 3.5 Ma. Earlier studies^[9] place the Miocene loess deposits into the so-called Gansu System. Our investigations show that the Gansu System contains indeed spatially coexisting sediments of various origins depending on paleo-topography. Eolian deposits were developed on highlands while waterlain deposits were formed within the depressions. The

eolian sequences of Miocene age reported in the recent years from Qinan^[7], Miziwan^[10] and from the high terraces near Xining^[11] suggest a wide-spread nature. This is also supported by the recent geochemical approaches showing that a significant proportion of the fine sediments within the lacustrine basins in the region was also derived from eolian dust materials^[12].

Up to date, the eolian origin of these pre-Quaternary loess deposits have been demonstrated by their geochemical properties^[7,8], the numerous paleosols^[7,8], the abundant land-snails and the lack of aquatic species^[13,14], morphology and grain-size of quartz^[7,15], spatially correlative stratigraphy and magnetic suscepti-

bility^[10]. However, systematic grain-size data have not yet been reported, which are of particular values for addressing the origin of the deposits^[16–19] and their paleoclimate significance^[20–24]. These are the main aims of the present report.

1 Materials and methods

The studied QA-I section (105°27'E, 35°02'N) is 253.1 m thick and is located 27 km northwest of Qinan City, Gansu Province^[7]. In this study, grain-sizes of 507 bulk samples at 50 cm intervals were analyzed. 10 loess and 9 soil samples of Quaternary age from the Xifeng site, 5 lacustrine samples from the Haiziping section^[25] in Luding county, Sichuan Province, and 8 fluvial samples from the lower portion of the Xuancheng section^[26], Anhui Province, were also analyzed for comparison. Samples were pretreated with hydrogen peroxide (H₂O₂) to remove the organic matter, then with hydrochloric acid (HCl) to remove the carbonates, and with sodium hexametaphosphate((NaPO₃)₆) for dispersion. Grain-size was determined using a Malvern Mastersizer 2000 particle analyzer with an analytical precision <1%.

2 Comparison of grain-size distributions of the Miocene loess, Quaternary loess, lacustrine and fluvial sediments

2.1 Grain-size distribution

Fig. 1(a), (b) and (c) illustrate the grain-size distributions of representative loess and soil samples from different depths of the QA-I section. The distributions are bimodal, with the silty fraction being dominant. The > 63 μm fraction represents a small amount. These are essentially similar to the grain-size distributions of the Quaternary loess (Fig. 1(d)), but differ from the multimodal patterns of the lacustrine (Fig. 1(e)) and fluvial (Fig. 1(f)) samples. Similar to the Quaternary loess-soil sequences (Fig. 1(d)), loess layers in the Miocene sequence are also regularly coarser than the soil layers (Fig. 1(a)–(c)), indicating colder-drier climate conditions for loess and warm-humid conditions for soils, as is the case for the Quaternary loess-soil sequences^[22].

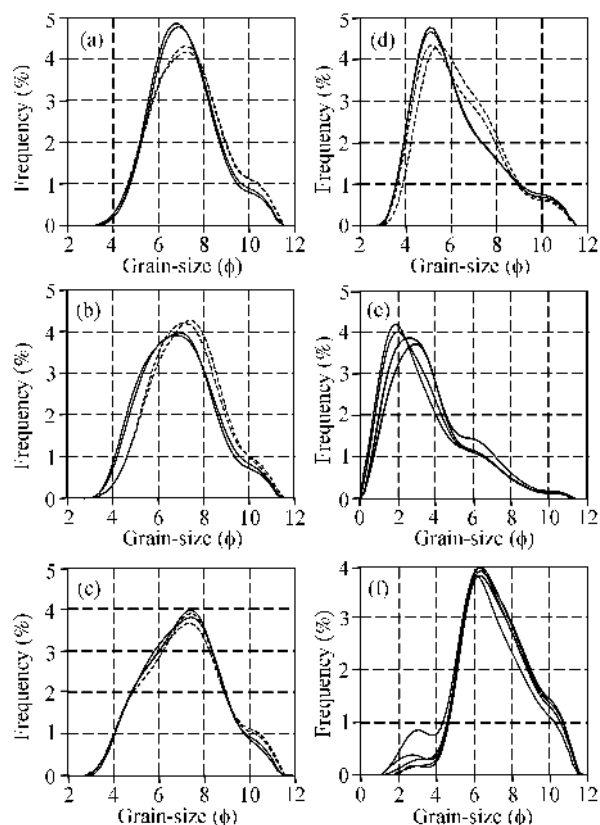


Fig. 1. Grain-size distribution curves of the Miocene and Quaternary loess and soil, lacustrine and fluvial samples. (a)–(c) Miocene loess and soil samples from the upper, middle and lower parts of the QA-I section, respectively (solid lines for loess samples and dotted lines for soil samples); (d) Quaternary loess and soil samples (solid lines for loess samples and dotted lines for soil samples); (e) lacustrine samples; (f) fluvial samples.

2.2 Grain-size parameters

Grain-size parameters are indicative of sedimentary environments and dynamical conditions^[27,28]. We calculate the values of mean, mean square deviation (MSD), skewness and kurtosis using the following equations^[27]:

$$\text{Mean} \quad \bar{X} = \frac{1}{100} \sum_{i=1}^n f_i X_i, \quad (1)$$

$$\text{MSD} \quad \sigma = \sqrt{\frac{1}{100} \sum_{i=1}^n (X_i - \bar{X})^2 f_i}, \quad (2)$$

$$\text{Skewness} \quad S = \sigma^{-3} \frac{1}{100} \sum_{i=1}^n (X_i - \bar{X})^3 f_i, \quad (3)$$

$$\text{Kurtosis} \quad K = \sigma^{-4} \frac{1}{100} \sum_{i=1}^n (X_i - \bar{X})^4 f_i. \quad (4)$$

X_i and f_i are the median grain-size and the content

of the fraction i . Comparisons of the grain-size parameters of the Miocene loess and soil samples, Quaternary loess and soil samples, the lacustrine and fluvial samples are shown in Fig. 2. The mean grain-size of the Miocene loess falls between 7.2ϕ and 6.5ϕ ($6.8-11.0 \mu\text{m}$), comparable to Quaternary soil samples, but finer than for Quaternary loess samples. The MSD values of Miocene and Quaternary loess are similar, but greatly differ from those of the lacustrine and fluvial samples, indicating a much better sorting and relatively stable depositional dynamics, characteristic of eolian dust deposits. Both Miocene and Quaternary loess and soil samples are positively skewed although the skewness values of the Miocene loess and soil samples are smaller than for the Quaternary loess and soil samples. The skewness values of the lacustrine samples are much larger. The kurtosis values of the Miocene loess and soil samples are close to those of the Quaternary loess and soil samples, smaller than for the lacustrine samples.

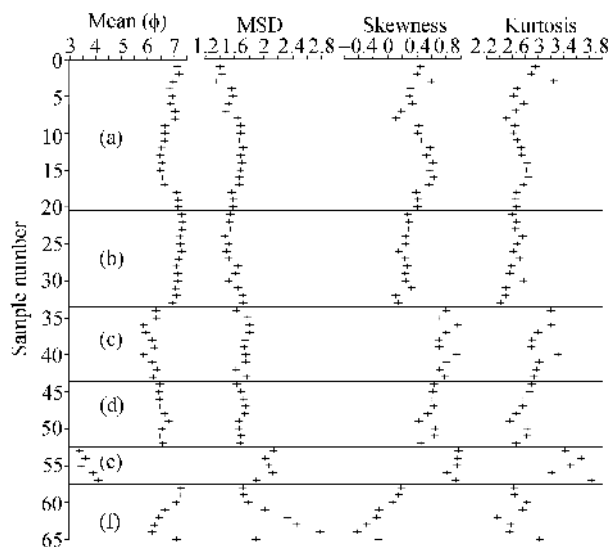


Fig. 2. Comparison of grain-size parameters for the Miocene loess (a) and soil (b) samples, Quaternary loess (c) and soil (d) samples, lacustrine (e) and fluvial (f) samples.

Although each grain-size parameter is dynamically significant, interpretation of sedimentary environments must be based on comprehensive analyses of the parameters. For this purpose, composite plots of mean, MSD, skewness and kurtosis are frequently used in sedimentological studies^[29]. Earlier comparisons of the composite plots showed a great similarity between

the late Miocene-Pliocene Red-Earth and the Quaternary loess and soil samples while those for lacustrine and fluvial sediments are quite different^[18,19]. Fig. 3 shows that the composite plots of the Miocene loess and soil samples are essentially comparable to those of the Quaternary loess and soil samples, but obviously different from the lacustrine and fluvial samples, supporting an eolian origin of the Miocene samples.

2.3 Q1-Md-Q3 plots

The Q1-Md-Q3 plots are used^[16] to separate samples of various depositional environments, in which Q1 and Q3 represent the grain-size corresponding to the cumulative contents of 75% and 25%, respectively. The Q1-Md-Q3 plots of the studied samples are shown in Fig. 4. The plots for the Miocene loess and soil samples are highly similar to those of the Quaternary loess and soil samples, but quite different from those of the lacustrine and fluvial sediments.

2.4 C-M plots

C-M plots are also frequently used to determine the sedimentary environments^[18,19,29], in which C and M represent the grain-size corresponding to the cumulative contents of 1% and 50% respectively. The C-M plots for the studied samples are shown in Fig. 5. The Miocene and Quaternary loess and soil samples are much closer and concentrated in the C-M pots (Fig. 5) within a belt roughly in parallel with the C-M baseline. Quaternary loess samples are coarser than for the Miocene samples. On the contrary, the plots for the lacustrine and fluvial samples are highly different from these eolian samples.

2.5 Empirical judgment

Empirical judgment is a statistical method to discriminate sediments of different sedimentary environments. In this study, the following equation^[30] is used:

$$Y = 3.5688 M_Z + 3.7016 \sigma_i^2 - 2.0766 K_Z + 3.1135 K_G. \quad (5)$$

The equation defines an index Y to discern sedimentary environments, in which M_Z , σ_i , K_Z , K_G are mean, MSD, skewness and kurtosis, respectively.

According to Sahu^[30], the Y -values of eolian depos-

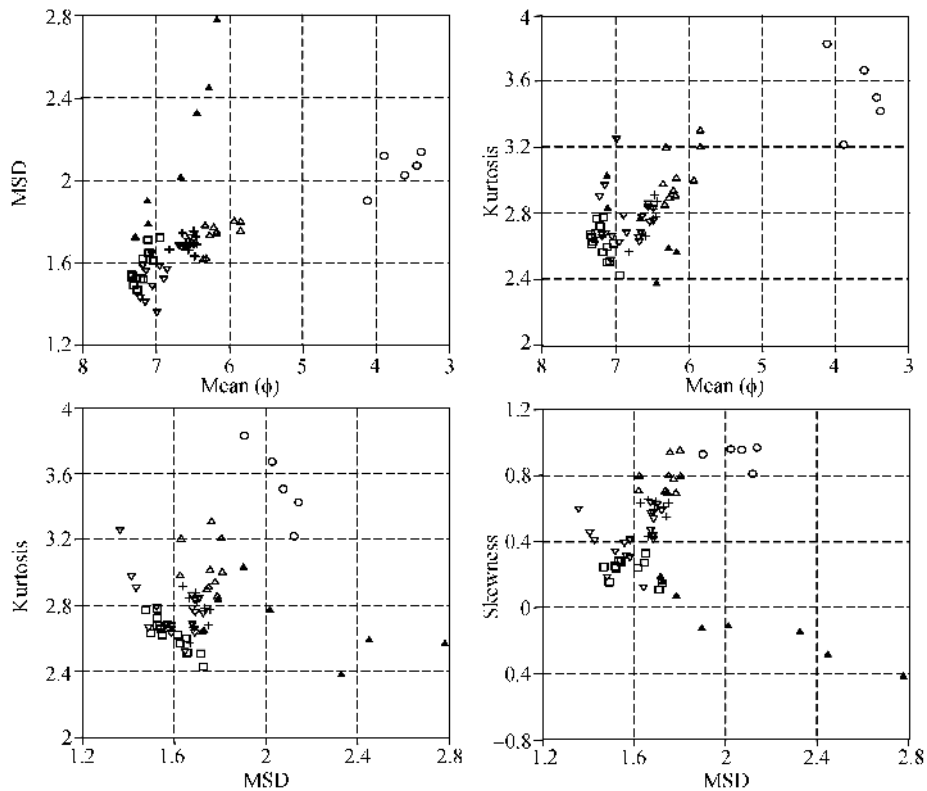


Fig. 3. Statistical parameters of grain-size distribution plots of the Miocene and Quaternary loess and soil, lacustrine and fluvial samples. ∇ , Miocene loess; \square , Miocene soil; \triangle , Quaternary loess; +, Quaternary soil; \circ , lacustrine sediment; \blacktriangle , fluvial sediment.

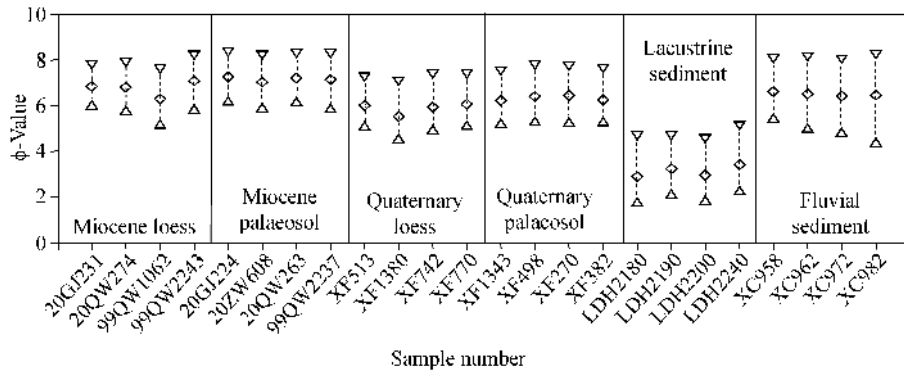


Fig. 4. Q1-Md-Q3 plots of the Miocene and Quaternary loess and soil, lacustrine and fluvial sediments. ∇ , Grain-size corresponding to the cumulative content of 75% (Q1); \triangle , grain-size corresponding to the cumulative content of 25% (Q3); \diamond , median grain-size (Md).

its using this equation should be smaller than -2.7411 . Fig. 6 shows that both the Miocene and Quaternary loess and soil samples are quite similar and fall into this range. Another prominent features of the Y -values for these eolian samples are the small variability, attributable to relatively stable dynamics. On the contrary, fluvial and lacustrine samples usually show

much larger ranges of Y -values due to the instability of sedimentary dynamics (Fig. 6). The studied fluvial samples yield negative values while some other fluvial samples may yield positive values^[18,19]. The much closer Y -values of the Miocene loess samples to those of the Quaternary loess, as well as their much narrow ranges strongly support an eolian origin.

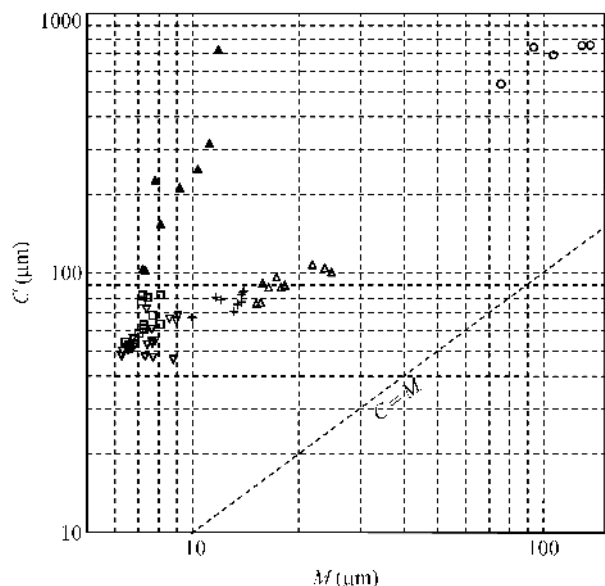


Fig. 5. *C-M* plots of the Miocene and Quaternary loess and soil, lacustrine and fluvial sediments. ∇ , Miocene loess; \square , Miocene soil; \triangle , Quaternary loess; $+$, Quaternary soil; \circ , lacustrine sediment; \blacktriangle , fluvial sediment.

2.6 Grain-size variations along the QA-I sequence

Variations of the median grain-size (*M*_d) and the content of different size fractions in the QA-I sequence are shown in Fig. 7. For all the analyzed samples, median grain-size varies from 6 to 13 μm . The content of the $>63 \mu\text{m}$ fraction accounts for 5.3% in maximum and represents only 0.9% in average. For a thick sequence of 253.1 m with a time span of about 16 Ma, these homogeneous grain-size variations must require exceptional stable sedimentary dynamics and are indeed only explainable by eolian dust deposits. Al-

though the presence of larger quartz grains (up to 1–2 mm) were noted during field descriptions within a few layers at the lower parts of the outcrops, they were not detected in this study because of their extremely scarce occurrence. This feature, usually observable in Quaternary loess sections over terraces, is attributable to local wind deflation or rain-splash transportation from the nearby highlands.

3 Long-term variations of grain-size and comparison with marine eolian records

In the studies of eolian deposits in northern China, grain-size is usually used as a proxy of the winter monsoon intensity, and loess accumulation rate is thought to be an indicator of aridity in the dust source regions^[20]. Later studies on the Quaternary loess-soil sequence^[31] and the *Hipparion* Red-Earth^[32] revealed that the variations of grain-size and accumulation rate are mostly coeval at over-orbital timescales.

Fig. 8 shows that the variations of grain-size (Fig. 8(a)) and accumulation rate (Fig. 8(b)) in the QA-I section are also approximately coeval, with coarser grain-size and higher accumulation rate for the intervals of 21.3–20.2 Ma, 16.0–13.3 Ma and 8.7–6.9 Ma. The peak of higher accumulation rate around 8 Ma has a clear counterpart in the records of eolian mass accumulation rate at Site 885/886 in the North Pacific^[33]. Because eolian accumulation rate in both marine and terrestrial records are considered an indication of aridity in the dust source areas^[20, 33], we believe that the Miocene eolian grain-size bears strong signals of continental aridity changes.

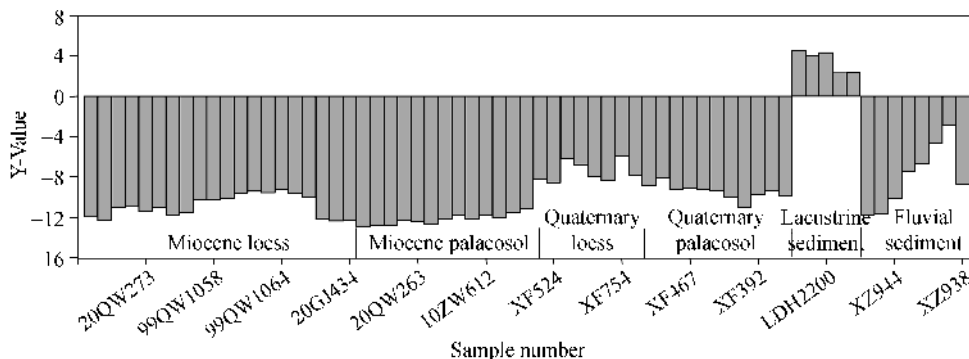


Fig. 6. *Y*-values of the grain-size distributions for the studied samples.

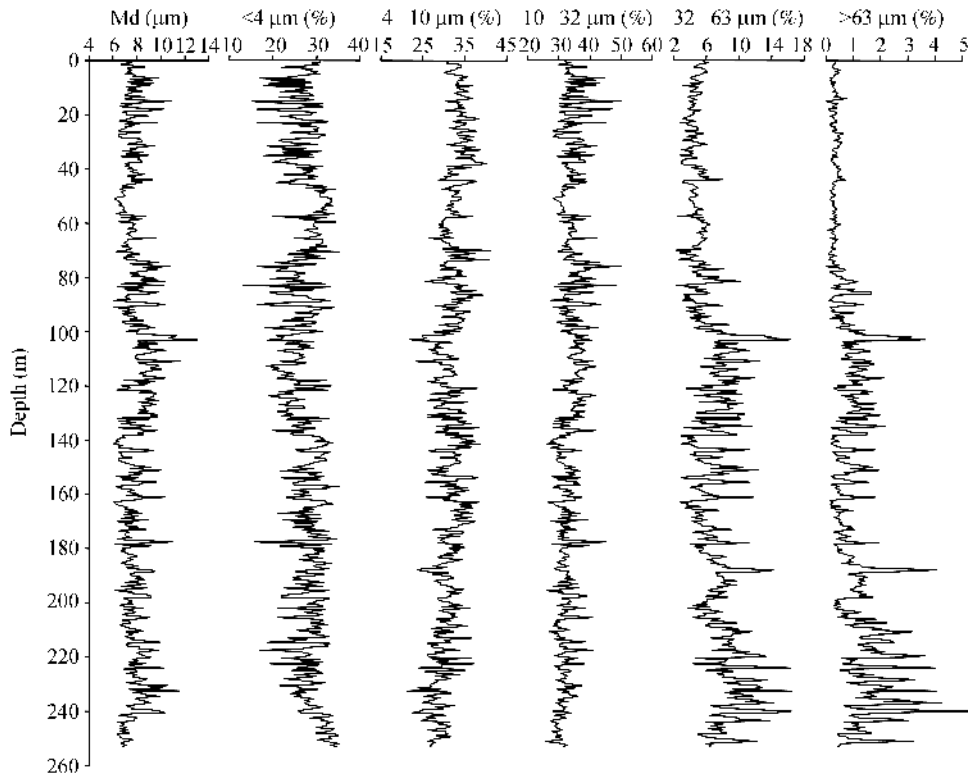


Fig. 7. Variations of median grain-size and contents of different fractions in the QA-I section.

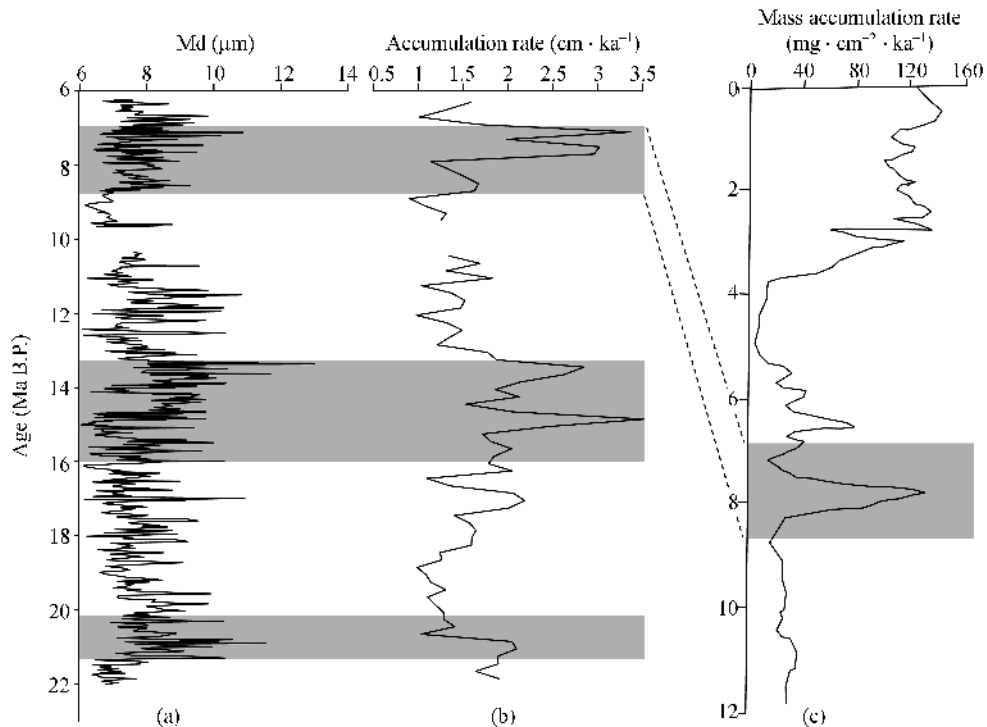


Fig. 8. Variations of grain-size (a) and loess accumulation rate (b) in the QA-I section and comparison with the eolian mass accumulation rate in the North Pacific (c). Timescale and loess accumulation rate of QA-I are from ref. [7]. The timescale was constructed using geomagnetic boundaries as age controls, interpolated using Kukla's magnetic susceptibility model^[34]. Data for eolian mass accumulation rate at Site 885/886 in the North Pacific are from ref. [33].

4 Conclusions

In this study, grain-size features of the QA-I Miocene loess-soil sequence are addressed and compared with those of the Quaternary loess and soil samples, representative lacustrine and fluvial samples. The results show that grain-size parameters of the Miocene loess and soil samples match well those of the typical Quaternary eolian samples, but greatly differ from those of the lacustrine and fluvial samples, as are strongly supportive to the eolian origin of the Miocene sequence.

For the entire 253.1 m section covering about 16 Ma, the content of the $>63 \mu\text{m}$ fraction accounts for 5.3% in maximum and represents only 0.9% in average. Silty fractions are constantly dominant with the median grain-size varying from 6 to $13 \mu\text{m}$. These features are characteristic of eolian dust deposits. Loess layers are regularly coarser than the soil layers in the Miocene sequence, as is also similar to the Quaternary loess-soil sequences, indicating cyclical changes of climate conditions.

At over-orbital timescales, the variations of grain-size in the Miocene loess-soil sequence are approximately coeval with loess accumulation rate. This suggests that grain-size variations in the Miocene loess-soil sequence are not only reflective to wind strength, but also to the aridity in dust source areas.

Acknowledgements This work was supported by the Chinese Academy of Sciences (Grant No. KZCX3-SW-139), the National Natural Science Foundation of China (Grant Nos. 40231001 and 40272088), and the “973” Project (Grant No. 2004CB720203).

References

- 1 Liu T S. Loess and the Environment (in Chinese). Beijing: Science Press, 1985
- 2 An Z S, Kutzbach J E, Prell S C, et al. Evolution of Asian monsoons and phased uplift of the Himalaya-Tibetan Plateau since Late Miocene times. *Nature*, 2001, 411: 62–66
- 3 Guo Z T, Peng S Z, Hao Q Z, et al. Origin of the Miocene-Pliocene Red-Earth Formation at Xifeng in northern China and implications for paleoenvironments. *Palaeogeogr Palaeoclimatol Palaeoecol*, 2001, 170: 11–26
- 4 Ding Z L, Sun J M, Liu T S, et al. Wind-blown origin of the Pliocene red clay formation in the central Loess Plateau, China. *Earth Planet Sci Lett*, 1998, 161: 135–143
- 5 Sun D H, Shaw J, An Z S, et al. Magnetostratigraphy and paleoclimatic interpretation of a continuous 7.2 Ma Late Cenozoic eolian sediments from the Chinese Loess Plateau. *Geophys Res Lett*, 1998, 25(1): 85–88
- 6 Qiang X K, Li Z X, Powell C, et al. Magnetostratigraphic record of the Late Miocene onset of the East Asian monsoon, and Pliocene uplift of northern Tibet. *Earth Planet Sci Lett*, 2001, 187: 83–93
- 7 Guo Z T, Ruddiman W F, Hao Q Z, et al. Onset of Asian desertification by 22 Myr ago inferred from loess deposits in China. *Nature*, 2002, 416: 159–163
- 8 Hao Q Z, Guo Z T. Magnetostratigraphy of a late Miocene-Pliocene loess-soil sequence in the western Loess Plateau in China. *Geophys Res Lett*, 2004, 31, L09209, doi: 10.1029/2003GL019392
- 9 Bureau of Geology and Miner Resources of Gansu Province. Regional Geology of Gansu Province (in Chinese). Beijing: Geological Publishing House, 1989. 298–302
- 10 Liu J F, Guo Z T, Hao Q Z, et al. Magnetostratigraphy of the Miziwan Miocene eolian deposits in Qin'an county (Gansu Province). *Quat Sci* (in Chinese), 2005, 25(4): 503–509.
- 11 Lu H Y, Wang X Y, An Z S, et al. Geomorphologic evidence of phased uplift of the northeastern Qinghai-Tibet Plateau since 14 Million years ago. *Sci China Ser D-Earth Sci*, 2004, 47(9): 822–833
- 12 Garzzone C N, Ikari M J, Basu A R. Source of Oligocene to Pliocene sedimentary rocks in the Linxia basin in northeastern Tibet from Nd isotopes: Implications for tectonic forcing of climate. *Geol Soc Amer Bull*, 2005, 117: 1156–1166
- 13 Li F J, Wu N Q, Pei Y P. Terrestrial mollusk evidence for the origin of a late Tertiary loess-paleosol sequence at Qin'an in the western Chinese Loess Plateau. *Quat Sci* (in Chinese), 2005, 25(4): 510–515
- 14 Li F J, Wu N Q, Rousseau D D. Preliminary study of mollusk fossils in the Qinan Miocene loess-soil sequence in western Chinese Loess Plateau. *Sci China Ser D-Earth Sci*, 2006, 49(7): 724–730
- 15 Liu J F, Guo Z T, Qiao Y S, et al. Eolian origin of the Miocene loess-soil sequence at Qin'an, China: Evidence of quartz morphology and quartz grain-size. *Chin Sci Bull*, 2006, 51(1): 117–120
- 16 Douglas D T. Grain-size indices, classifications and environment. *Sedimentology*, 1968, 10: 132–152
- 17 Visher G S. Grain size distribution and depositional process. *J Sedimen Petrol*, 1969, 39: 1074–106
- 18 Lu H Y, Vandenberghe, An Z S. Aeolian origin and paleoclimatic implications of the ‘Red Clay’ (north China) as evidenced by grain-size distribution. *J Quat Sci*, 2001, 16(1): 89–97
- 19 Lu H Y, An Z S. Comparison of grain-size distribution of red

- clay and loess-palaeosol deposits in Chinese Loess Plateau. *Acta Sediment Sin (in Chinese)*, 1999, 17(2): 226—232
- 20 An Z S, Kukla G, Porter J L, et al. Late Quaternary dust flow on the Chinese Loess Plateau. *Catena*, 1991, 19: 171—187
- 21 An Z S. The history and variability of the East Asian paleomonsoon climate. *Quat Sci Rev*, 2000, 19: 171—187
- 22 Ding Z L, Yu Z W, Rutter N W, et al. Towards an orbital time scale for Chinese Loess deposits. *Quat Sci Rev*, 1994, 13: 39—70
- 23 Xiao J L, Potter S C, An Z S, et al. Grain size of quartz as an indicator of winter monsoon strength on the Loess Plateau of central China during the last 130,000yr. *Quat Res*, 1995, 43: 22—29
- 24 Lu H Y, An Z S. Paleoclimatic significance of grain size of loess-palaeosol deposit in Chinese Loess Plateau. *Sci China Ser D-Earth Sci*, 1998, 41(6): 626—631
- 25 Jiang F C, Wu X H. Late Cenozoic tectonic movement in geomorphologic boundary belt of southeastern Qinghai-Xizang Plateau. *J Chengdu Univ Tech (in Chinese)*, 1998, 25(2): 162—168
- 26 Qiao Y S, Guo Z T, Hao Q Z, et al. Loess-soil sequences in southern Anhui Province: Magnetostratigraphy and paleoclimatic significance. *Chin Sci Bull*, 2003, 48(19): 2088—2093
- 27 Friedman G M, Sanders J E. *Principles of Sedimentology*. New York: John Wiley & Sons, 1978. 792
- 28 Folk R L, Ward W C. Brazos river bar: A study in significance of grain size parameters. *J Sediment Petrol*, 1957, 27(1): 3—26
- 29 Passega R. Grain size representation by CM pattern as a geologic tool. *J Petrol*, 1964, 34: 830—847
- 30 Sahu B K. Depositional mechanism from the size analysis of clastic sediments. *J Sediment Petrol*, 1964, 34: 337—343
- 31 Ding Z L, Yu Z W, Yang S L, et al. Coeval changes in grain size and sedimentation rate of eolian loess, the Chinese Loess Plateau. *Geophys Res Lett*, 2001, 28(10): 2097—2100
- 32 Guo Z T, Peng S Z, Hao Q Z, et al. Late Miocene-Pliocene development of Asian aridification as recorded in the Red-Earth Formation in northern China. *Glob Planet Change*, 2004, 41: 135—145
- 33 Rea D K, Snoeckx H, Joseph L H. Late Cenozoic eolian deposition in the North Pacific: Asian drying, Tibetan uplift, and cooling of the Northern Hemisphere. *Paleoceanography*, 1998, 13(3): 215—224
- 34 Kukla G, Heller F, Liu X M, et al. Pleistocene climates in China dated by magnetic susceptibility. *Geology*, 1988, 16: 811—814